Crustal resistivity structure at 9°50′N on the East Pacific Rise: Results of an electromagnetic survey

Rob L. Evans,[1] Spahr C. Webb,[2] and the RIFT-UMC Team[3]

Received 20 September 2001; revised 17 November 2001; accepted 2 January 2002; published 21 March 2002.

[1] We report the first results of an extensive electromagnetic survey of the East Pacific Rise (EPR) at 9°50′N, which used the magnetometric resistivity (MMR) technique to measure the electrical resistivity structure of the seafloor in the vicinity of the spreading center. Ten seafloor magnetometers were deployed in areas of known hydrothermal activity, in axial sites devoid of venting, and further off-axis to a distance of approximately 4 km. Data collected at off-axis sites show higher seafloor resistivities than at axial sites. This response is opposite to that expected from porosity controlled resistivity structure, with a thicker high-porosity extrusive layer 2A off-axis, as required by seismic data. An explanation for the reduced axial resistivities is that the uppermost few hundred meters of crust are much hotter beneath the ridge crest than a few kilometers off-axis, lowering the pore-fluid resistivity. *INDEX TERMS:* 3035 Marine Geology and Geophysics: Midocean ridge processes; 3015 Marine Geology and Geophysics: Heat flow (benthic) and hydrothermal processes; 3094 Marine Geology and Geophysics: Instruments and techniques

1. Introduction

[2] The porosity and permeability structure of the oceanic crust, the fundamental physical properties which control hydrothermal circulation and regulate its behavior both in time and space [e.g. *Rosenberg et al.*, 1993], are poorly known. Variations in crustal structure beneath midocean ridges have been measured by a variety of geophysical techniques, most notably through seismic reflection, refraction and tomography. Changes in velocity structure along the ridge crest and across discontinuities in axial structure have been identified as thermal anomalies resulting from variations in patterns of hydrothermal circulation [*Toomey et al.*, 1994; *Tian et al.*, 2000], while changes in velocity structure away from ridge axes have been explained in terms of differences in thickness of the uppermost extrusive layer of oceanic crust [*Harding et al.*, 1993]. While seismic velocity is dependent on the thermal structure of the crust itself, it is not dependent on the temperature or salinity of circulating fluids. On the other hand, the electrical resistivity of the seafloor is sensitive primarily to the amount of seawater within the crust, how it is distributed, and its temperature and salinity. Because of this sensitivity, measurements of seafloor electrical resistivity can be used to infer patterns of hydrothermal circulation in the shallow crust, provided that a suitable experimental geometry is utilized.

[1]Woods Hole Oceanographic Institution, USA.
[2]Lamont Doherty Earth Observatory, USA.
[3]RIFT-UMC Team: W. Crawford, IPGP, Paris; C. Golden, MPL, Scripps Institution of Oceanography; K. Key, IGPP, Scripps Institution of Oceanography; L. Lewis, Arnold Orange Associates, Houston, TX; H. Miyano, Chiba University, Japan; E. Roosen, Dept. of Geology and Geophysics, Woods Hole Oceanographic Inst; D. Doherty, Scripps Institution of Oceanography.

0094-8276/02/2001GL014106$05.00

[3] The MMR method is a logistically simple magnetic technique that involves two components: a vertical bipole source; and separate seafloor magnetometers as receivers [*Edwards et al.*, 1981]. The method does not rely on induction, yet it differs from standard resistivity soundings because it can resolve the structure of a resistive seafloor under a more conductive ocean [*Nobes et al.*, 1986; *Evans et al.*, 1998]. In the presence of a layered Earth, the magnetic field generated by a bipole source is azimuthally symmetric and "falls-off" with distance from the source approximately as $1/r^2$ [*Edwards et al.*, 1981]. The amplitude of the magnetic field at the receiving site can be used to estimate the electrical resistivity of the seafloor. Experience has shown that the depth of resolution of the technique is about 1/3 the maximum source-receiver offset.

[4] Here, we report on the largest seafloor MMR experiment carried out to date. We deployed 10 seafloor magnetometers across the axis of the EPR at 9°50′N. Magnetometers were placed in a variety of settings: close to high temperature vents; on-axis but removed from active venting; and further off-axis (Figure 1). We transmitted to these magnetometers from 200 locations, providing source-receiver separations in excess of 5 km on all instruments.

2. Structure of the EPR at 9°50′N

[5] The section of EPR between the Clipperton and Siqueiros transform faults has been widely studied, with a substantial amount of work focused around 9°50′N. It is well known that a ~500 m wide melt body underlies most of the ridge at a depth of about 1.5 km [*Detrick et al.*, 1987; *Kent et al.*, 1993] and is more or less continuous along strike, indicating a high degree of magmatic robustness. Near bottom camera tows have mapped venting and fissuring in and around the neovolcanic zone [*Haymon et al.*, 1991, 1993; *Wright et al.*, 1995]. The segment of ridge between 9°45′N and 9°52′N contains a large number of high temperature vents, most of which are found towards the ends of the segment. The segment is also known to have erupted in 1991 resulting in an increase in hydrothermal venting activity [*Haymon et al.*, 1993]. A suggested model for the high temperature component of flow consists of recharge in the adjacent ridge segments to the south and north, ridge parallel flow extending into the dike complex, and focused high temperature venting at the ends of the segment [*Rosenberg et al.*, 1993].

[6] A small aperture seismic tomography experiment at 9°50′N shows evidence for along-axis variations in crustal thermal structure linked with a fourth order ridge axis discontinuity at 9°52′N [*Tian et al.*, 2000]. North of the discontinuity, where hydrothermal venting is absent, upper crustal velocities are raised, consistent with a cooler thermal structure. An along-axis temperature variation of about 300°C within the sheeted dike complex can explain the difference in velocities across the discontinuity. Finally, a series of micro-earthquakes observed by ocean bottom seismometers has been interpreted as the result of thermal cracking induced by fluids mining heat from the conductive thermal boundary layer overlying the magma chamber [*Sohn et al.*, 1999, 1998]. The earthquake locations constrain

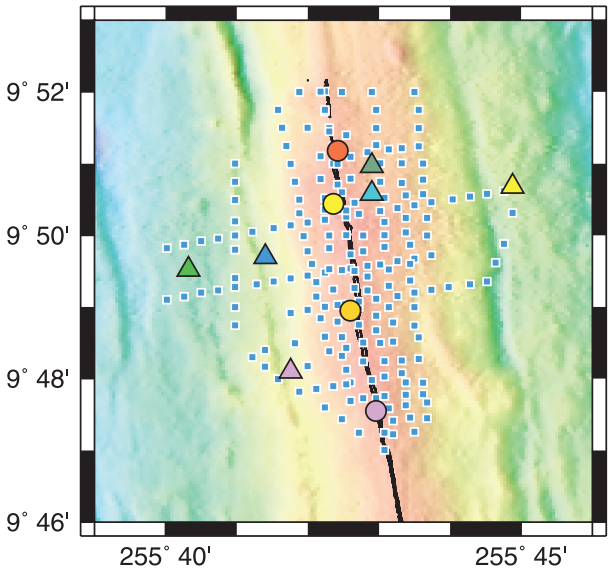

Figure 1. A map of bathymetry across the EPR at 9°50′N showing locations of our ten ocean bottom magnetometers (colored circles and triangles) and the more than 200 transmission stations (blue squares) completed during our experiment.

the 450°C isotherm to a depth of approximately 1100 m below seafloor.

3. Experiment and Data

[7] Transmission consisted of occupying a station for 30 minutes. During this time a square wave with an approx. 13 s period and with a peak current of 13 A was passed between an electrode at the sea surface and one just above the seafloor on the end of the 0.680 coax conductor ship's wire. Transmitting a square-wave allows easy identification of the transmitted harmonics above the ambient magnetic field variations.

[8] Magnetic fields were recorded on two kinds of instruments [*Webb et al.*, 2001; *Constable et al.*, 1998]. Precise positions for all the seafloor instruments were determined from acoustic surveying. The position of the ship was dynamically maintained during transmission to within 50 m of the station location.

[9] Amplitudes of the transmitted magnetic fields were determined for the transmission time-windows (Figure 2). Noise levels on each instrument were determined by analysis of non-transmission data windows. If the seafloor resistivity were a function of depth only, then data from each receiver would be indistinguishable from each other. In fact, we see significant differences in amplitude behavior between receivers. Most striking are the lower amplitudes seen on instruments further from the ridge crest, indicating more resistive structure a few km off-axis within the uppermost crust. All the axial instruments show higher amplitudes, and a lower degree of variability than amplitudes on off-axis instruments, both between instruments and between amplitudes on a single instrument. Amplitudes from all instruments are similar at ranges greater than about 4 km. To clarify these differences, we have averaged amplitudes from several instruments in 500 m range bins (Figure 3a).

[10] Simple 1-D smooth inversions [*Constable et al.*, 1987] of representative data from on-axis and a site 4 km to the west reveal the differences in resistivity structure between zero age and approx. 100,000 year old crust (Figure 3c). Both models show low resistivity near the seafloor consistent with high shallow porosities. The on- and off-axis models differ greatly near 300 m depth, with the on-axis sites much less resistive. The two models converge again near 1 km depth, corresponding to the convergence in the magnetic field amplitudes at ranges >4 km. While the act of averaging amplitudes is useful to exemplify first order differences between instruments, it removes the more subtle, and potentially important, variations in amplitude that arise from spatial variations in resistivity structure. Understanding the entire resistivity structure across the ridge-crest, including the potential effects of localised hydrothermal circulation and of the axial magma-chamber, will require a full 3-D treatment of the amplitude data that will be the subject of future research. For example, long-range transmissions sample larger volumes of seafloor, and also include transmissions both along and across the ridge crest. The effect of a deep conductor associated with an axial magma chamber could be significant for these data and not obvious to identify. Until this is done, we cannot be sure of structure below ~1 km depth, where seismic and thermal models show evidence for strong lateral variations in temperature and melt content.

4. Discussion

[11] Seismic data show clear evidence for a thickening of layer 2A away from the ridge crest at 9°50′N. This layer has low seismic velocities, and is usually interpreted to be rubbly, high-porosity, extrusives. Models of 2A formation also include a higher percentage of low-porosity dikes near the seafloor on axis [*Hooft et al.*, 1996]. Yet our data show lower resistivities near the seafloor on axis where shallow porosity is lower.

[12] There is substantial ambiguity in interpreting resistivity profiles in terms of temperature and porosity. Competing first order processes occur in the uppermost few hundred meters of seafloor that can impact the resistivity and cause changes in structure with distance away from the ridge: These include (1) pore-water cooling which increases its resistivity (2) layer 2A thickening resulting in changes in porosity with depth and with distance away from the axis (3) alteration and crack closure which reduce bulk porosity making the crust more resistive. Alteration can have two effects on resistivity: it lowers overall porosity and it

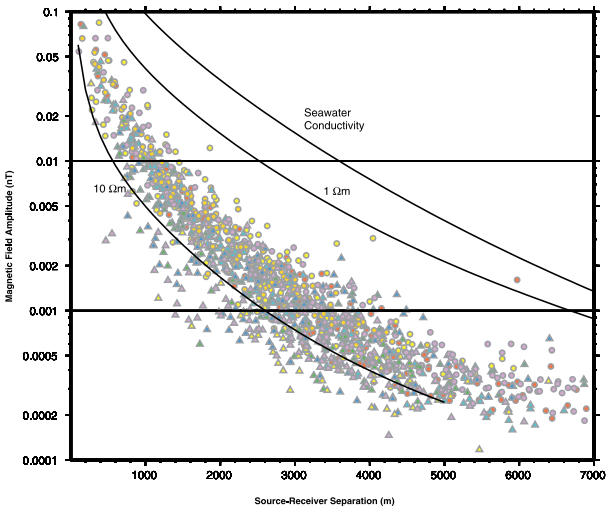

Figure 2. Magnetic field amplitude data for all instruments. Amplitudes for each receiver are shown using the same color symbol used for receiver location in Figure 1, with circles for the ridge crest instruments and triangles for those off-axis. If the underlying seafloor were a uniform layered structure, amplitudes from different receivers would plot along the same amplitude versus range curve. The effect of differing seafloor resistivity is shown by the 1/2 space curves as labelled.

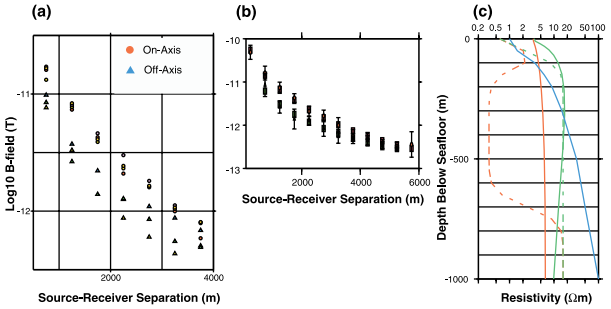

Figure 3. (a) Amplitudes for instruments sited along and off-axis averaged in 500 m range bins (symbols as per Figure 2). Instruments on the ridge crest (circles) recorded higher magnetic field amplitudes to source-receiver distances of about 4 km, consistent with more conductive crust beneath the ridge crest. (b) Binned data from a ridge crest site (red circles) and the westernmost site away from the ridge (green triangles) with the fit to each (squares) for the resistivity models of (c) (solid red (on-axis) and green (off-axis)). Models for the EPR at 13°N (blue) [*Evans et al.*, 1991] and for axial (red-dashed) and off-axis (green dashed) JDF [*Evans et al.*, 1998] are also shown.

might also reduce the pore-space connectivity reducing the effectiveness of seawater as a conductive phase [*Gillis and Sapp*, 1997].

[13] We explain the lower axial resistivities by the presence of hotter pore-fluids beneath the ridge crest, offsetting the effects of porosity. The similarity in resistivity at depths around 1 km on- and off-axis points to a uniform temperature and porosity structure in the sheeted dike complex across the ridge to distances of at least 5 km. The low resistivities in our axial model do not suggest that our data have measured a region of seafloor with fluid temperatures greater than 350°C. This may be a resolution issue, with the effects of a thin resistive layer around 1 km, offset by the deeper conductive magma body. We also note that in the Lau basin [*MacGregor et al.*, 2001] saw similarly low resistivities beneath the Valu Fa Ridge to depths of 3 km.

[14] Electrical resistivity profiles measured at 9°50′N are different to, and generally less resistive than, those measured further north at 13°N (Figure 3c). A steep resistivity gradient was observed at 13°N, with significantly higher resistivities seen at depths around 1 km. Also, no difference in structure was seen between zero age and 100,000 year old crust (*Evans et al.*, 1991). In general, the structure at 13°N is consistent with high porosities near the seafloor falling rapidly to less than 1% around 1 km, with little evidence for substantial layer 2A thickening away from the ridge crest. These models are also consistent with fairly low crust and fluid temperatures, supporting the idea that the section of ridge immediately north of 13°N is magmatically quiescent and has been extensively cooled by circulating fluids.

[15] Another MMR experiment in the Cleft-Vance overlapping spreading center on the JDF, showed even lower axial resistivities (but similar off-axis structure) within the uppermost 600–800 m of crust associated with a recent shallow dike intrusion event and subsequent high temperature fluid circulation [*Evans et al.*, 1998] (Figure 3c). This is despite the fact that the EPR at 9°50′N is significantly more hydrothermally active than the Cleft segment. One explanation for this is that hot fluids flow in spatially limited fissures on the EPR and have less impact on the bulk resistivity, whereas at Cleft the seafloor is more extensively faulted distributing hot fluids over a larger volume of seafloor.

[16] **Acknowledgments.** We would like to thank the captain and crew of the R/V Melville for all their assistance during the RIFT-UMC cruise. Funding for the experiment was provided by NSF grant OCE-9819260. Maurice Tivey and two anonymous reviewers are thanked for their comments on the manuscript.

References

Constable, S. C., R. L. Parker, and C. G. Constable, Occam's inversion: A practical algorithm for generating smooth models from electromagnetic sounding data, *Geophysics*, *52*, 289–300, 1987.

Constable, S., A. Orange, G. M. Hoversten, and H. F. Morrison, Marine magnetotellurics for petroleum exploration Part 1. A seafloor instrument system, *Geophysics*, *63*, 816–825, 1998.

Detrick, R. S., P. Buhl, E. Vera, J. Mutter, J. Orcutt, J. Madsen, and T. Brocher, Multi-Channel seismic imaging of a crustal magma chamber along the East Pacific Rise, *Nature*, *326*, 33–41, 1987.

Edwards, R. N., L. K. Law, and J. M. Delaurier, On measuring the electrical conductivity of the oceanic crust by a modified magnetometric resistivity method, *J. Geophys. Res.*, *86*, 11,609–11,615, 1981.

Evans, R. L., S. C. Constable, M. C. Sinha, C. S. Cox, and M. J. Unsworth, Upper-crustal resistivity structure of the East Pacific Rise near 13°N, *Geophys. Res. Letts.*, *18*, 1917–1920, 1991.

Evans, R. L., S. C. Webb, R. N. Edwards, M. Jegen, and K. Sananikone, Hydrothermal Circulation at the Cleft-Vance Overlapping Spreading Centre: Results of a Magnetometric Resistivity Survey, *J. Geophys. Res.*, *103*, 12,321–12,338, 1998.

Gillis, K. M., and K. Sapp, Distribution of porosity in a section of upper oceanic crust exposed in the Troodos ophiolite, *J. Geophys. Res.*, *102*, 10,133–10,149, 1997.

Harding, A. J., G. M. Kent, and J. A. Orcutt, A multichannel seismic investigation of the upper crustal structure at 9°N on the East Pacific Rise: implications for crustal accretion, *J. Geophys. Res.*, *98*, 13,925–13,944, 1993.

Haymon, R. M., D. J. Fornari, M. H. Edwards, S. Carbotte, D. Wright, and K. C. Macdonald, Hydrothermal vent distribution along the East Pacific Rise crest (9°09′–54′N) and its relationship to magmatic and tectonic processes on fast spreading mid-ocean ridges, *Earth Planet. Sci. Letts.*, *104*, 513–534, 1991.

Haymon, R. M., D. J. Fornari, K. L. Von Damm, M. D. Lilley, M. R. Perfit, J. M. Edmond, W. C. Shanks, R. A. Lutz, J. M. Grebmeier, S. Carbotte, D. Wright, E. McLaughlin, M. Smith, N. Beedle, and E. Olson, Volcanic eruption of the midocean ridge along the East Pacific Rise crest at 9°45–52′N: direct submersible observations of seafloor phenomena associated with an eruption event in April 1991, *Earth Planet. Sci. Letts.*, *119*, 85–101, 1993.

Hooft, E. E. E., H. Schouten, and R. S. Detrick, Constraining crustal emplacement processes from the variation in seismic layer 2A thickness at the East Pacific Rise, *Earth Planet. Sci. Letts.*, *142*, 289–309, 1996.

Kent, G. M., A. J. Harding, and J. A. Orcutt, Distribution of magma beneath the East Pacific Rise between the Clipperton transform and 9°17′N Deval from forward modeling of common depth point data, *J. Geophys. Res.*, *98*, 13,945–13,969, 1993.

MacGregor, L., M. Sinha, and S. Constable, Electrical resistivity structure of the Valu Fa Ridge, Lau Basin, from marine controlled source electromagnetic sounding, *Geophys. J. Int.*, *146*, 217–236, 2001.

Nobes, D. C., L. K. Law, and R. N. Edwards, The determination of resistivity and porosity of the sediment and fractured basalt layers near the Juan de Fuca Ridge, *Geophys. J. R. Astr. Soc.*, *86*, 289–317, 1986.

Rosenberg, N. D., F. J. Spera, and R. M. Haymon, The relationship between flow and permeability field in seafloor hydrothermal systems, *Earth Planet. Sci. Lett.*, *116*, 135–153, 1993.

Sohn, R. A., D. J. Fornari, K. L. Von Damm, J. A. Hildebrand, and S. C. Webb, Seismic and hydrothermal evidence for a cracking event on the East Pacific Rise crest at 9°50′N, *Nature*, *396*, 159–161, 1998.

Sohn, R. A., J. A. Hildebrand, and S. C. Webb, A micro-earthquake survey of the high-temperature vent fields on the volcanically active EPR (9°50′N), *J. Geophys. Res.*, *104*, 25,367–25,377, 1999.

Tian, T., W. S. D. Wilcock, D. R. Toomey, and R. S. Detrick, Seismic heterogeneity in the upper crust near the 1991 eruption site on the EPR, 9°50′N, *Geophys. Res. Letts.*, *27*, 2369–2372, 2000.

Toomey, D. R., S. C. Solomon, and G. M. Purdy, Tomographic imaging of the shallow crustal structure of the East Pacific Rise at 9°30′N, *J. Geophys. Res.*, *99*, 24,135–24,157, 1994.

Webb, S. C., T. K. Deaton, and J. C. Lemire, A broadband ocean-bottom seismometer system based on a 1 Hz natural period geophone, *Bull. Soc. Seism. Amer.*, *91*(2), 304–312, 2001.

Wright, D. J., R. M. Haymon, and D. J. Fornari, Crustal fissuring and its relationship to magmatic and hydrothermal processes on the East Pacific Rise crest (9°12′ to 54′N), *J. Geophys. Res.*, *100*, 6097–6120, 1995.

R. L. Evans, Dept. of Geology and Geophysics, Woods Hole Oceanographic Institution, Woods Hole, MA 02543. (revans@whoi.edu)

S. C. Webb, Lamont Doherty Earth Observatory, 61 Route 9W Palisades, NY 10964. (scw@ldeo.columbia.edu)